Electronic Supplementary Material (ESI) for Journal of Materials Chemistry C.

Supporting Information

Stacked Perovskite photo detectors for multi-color fluorescence detection

Kai Zheng, Longkai Yang, Haowei Liu, Jiaqin Wang, Jingqin Cui, Xinyi Chen, Xin Li, Miao Lu**
Pen-Tung Sah Research Institute of Micro-Nano Science & Technology, Xiamen University, Xiamen 361005, P.R. China * lixin01@xmu.edu.cn lm@xmu.edu.cn

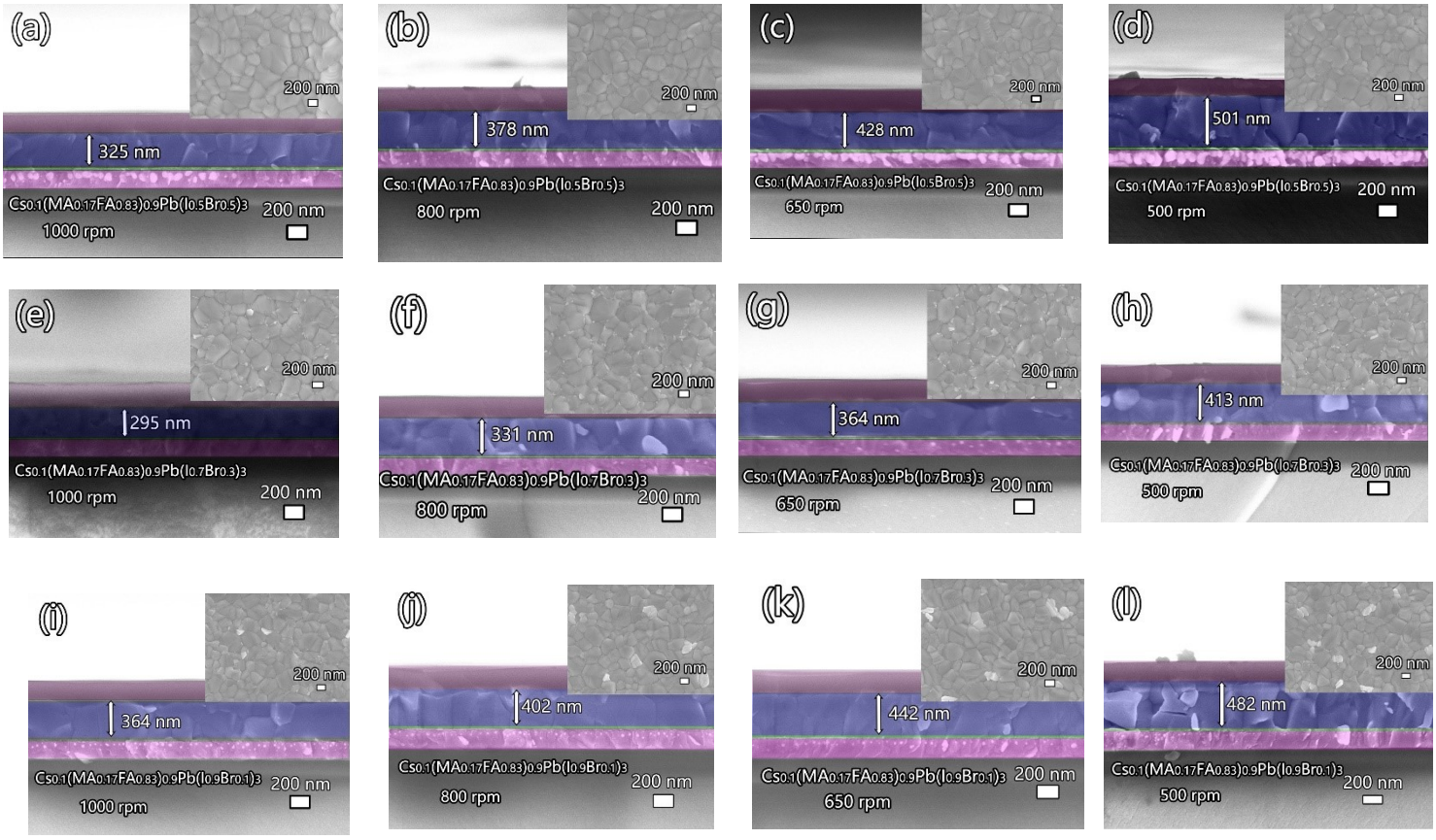

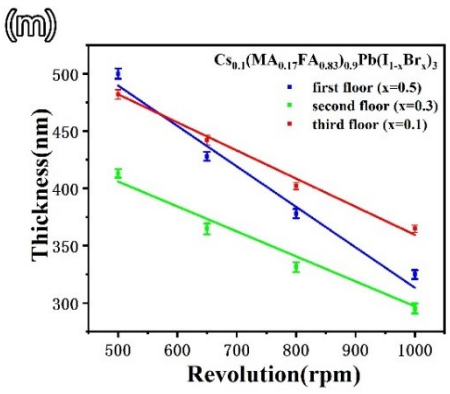

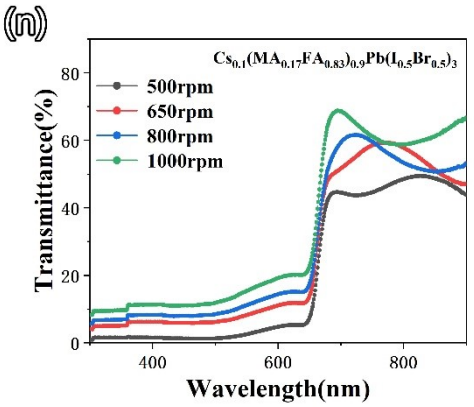

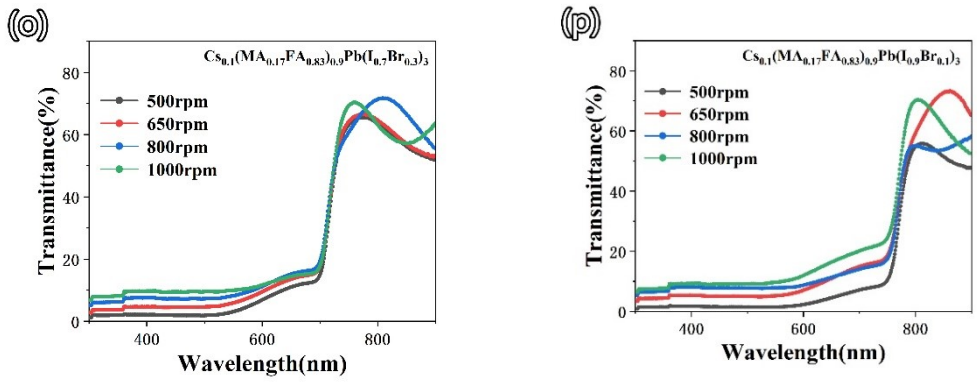

Fig. S1. SEM images of the cross-section morphology and the surface morphology of the $Cs_{0.1}(MA_{0.17}FA_{0.83})_{0.9}Pb(I_{0.5}Br_{0.5})_3$ TCPP with different spin-coating rate: (a) 1000 rpm, (b) 800 rpm, (c) 650 rpm, (d) 500 rpm. SEM images of the cross-section morphology and the surface morphology of the $Cs_{0.1}(MA_{0.17}FA_{0.83})_{0.9}Pb(I_{0.7}Br_{0.3})_3$ TCPP with different spin-coating rate: (e) 1000 rpm, (f) 800 rpm, (g) 650 rpm, (h) 500 rpm. SEM images of the cross-section morphology and the surface morphology of the $Cs_{0.1}(MA_{0.17}FA_{0.83})_{0.9}Pb(I_{0.9}Br_{0.1})_3$ TCPP with different spin-coating rate: (i) 1000 rpm, (j) 800 rpm, (k) 650 rpm, (l) 500 rpm. (m) Relationship between the thickness of perovskite layer and spin-coating rate of $Cs_{0.1}(MA_{0.17}FA_{0.83})_{0.9}Pb(I_{1-x}Br_x)_3$ (x=0.5, 0.3, 0.1). UV-vis transmittance spectra of $Cs_{0.1}(MA_{0.17}FA_{0.83})_{0.9}Pb(I_{1-x}Br_x)_3$ films prepared from precursor solution with different spin-coating rate (500 to 100 rpm), (n) x=0.5, (o) x=0.3, (p) x=0.1.

$Cs_{0.1}(MA_{0.17}FA_{0.83})_{0.9}Pb(I_{1-x}Br_x)_3$, (x=0.5, 0.3, 0.1) films were spin-coated at 500, 650, 800, and 1000 rpm, respectively, and their SEM image of the cross-section morphology and the surface morphology and UV-vis transmittance spectra were measured. The result suggested that the transmittance of short-wavelength bands was reduced to near zero when the spinning rate decreased to 500 rpm.

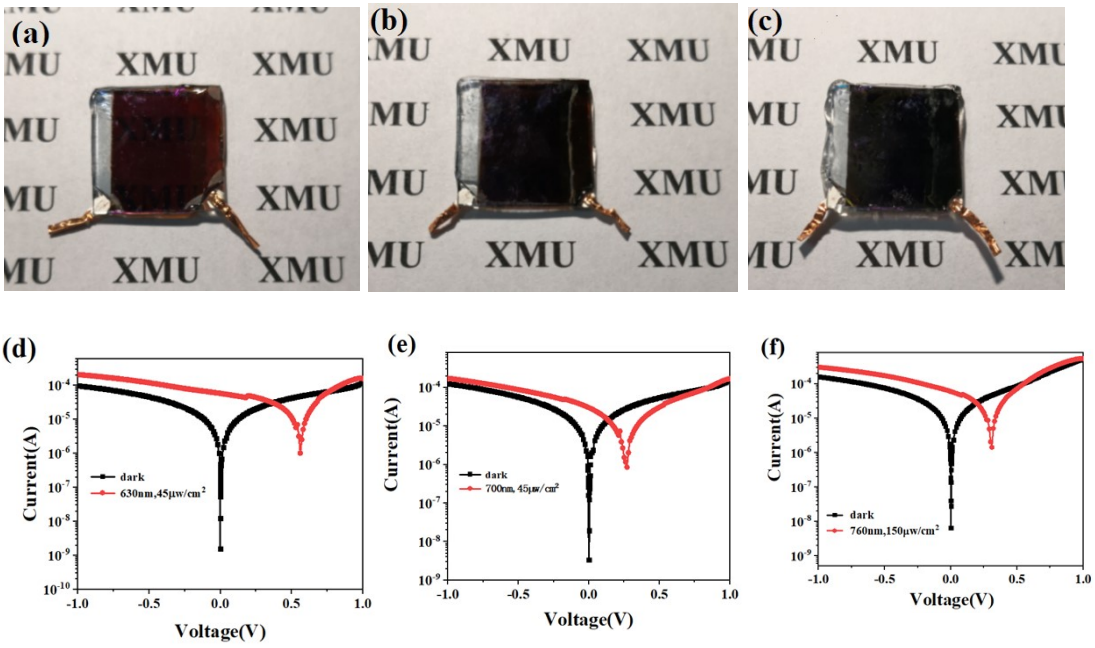

Fig. S2. Photographs of (a) $Cs_{0.1}(MA_{0.17}FA_{0.83})_{0.9}Pb(I_{0.5}Br_{0.5})_3$, (b) $Cs_{0.1}(MA_{0.17}FA_{0.83})_{0.9}Pb(I_{0.7}Br_{0.3})_3$ and (c) $Cs_{0.1}(MA_{0.17}FA_{0.83})_{0.9}Pb(I_{0.9}Br_{0.1})_3$ TCPP. The I-V characteristics of (d) $Cs_{0.1}(MA_{0.17}FA_{0.83})_{0.9}Pb(I_{0.5}Br_{0.5})_3$TCPP under 630 nm light (45 μw/cm^2), (e) $Cs_{0.1}(MA_{0.17}FA_{0.83})_{0.9}Pb(I_{0.7}Br_{0.3})_3$TCPP under 700 nm light (45 μw/cm^2), (f) $Cs_{0.1}(MA_{0.17}FA_{0.83})_{0.9}Pb(I_{0.9}Br_{0.1})_3$TCPP under 760 nm light (150 μw/cm^2)

The photoelectric response of three TCPP devices, $Cs_{0.1}(MA_{0.17}FA_{0.83})_{0.9}Pb(I_{0.5}Br_{0.5})_3$ TCPP, $Cs_{0.1}(MA_{0.17}FA_{0.83})_{0.9}Pb(I_{0.7}Br_{0.3})_3$ TCPP and $Cs_{0.1}(MA_{0.17}FA_{0.83})_{0.9}Pb(I_{0.9}Br_{0.1})_3$ TCPP under 630 nm, 700 nm, and 760 nm illumination respectively were given. It showed the photocurrents of the three kinds of TCPP all increased by approximately four orders of magnitude compared with the dark current at the zero bias.

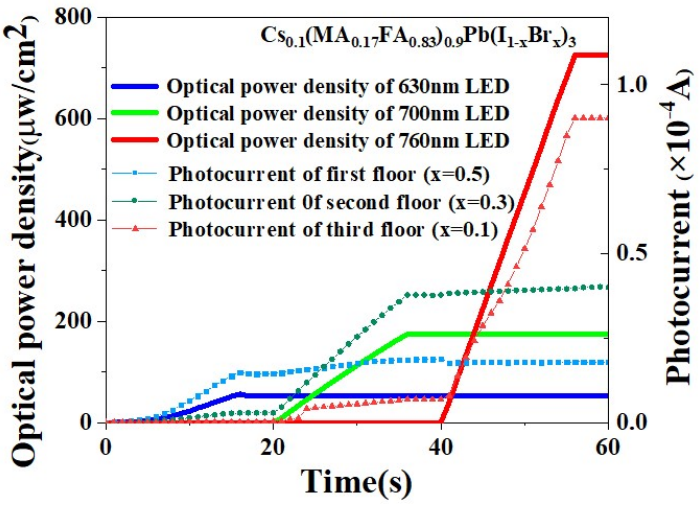

Fig. S3. The time dependent input optical power densities and the corresponding photocurrents of SPSD. Three LEDs of the central wavelength 630, 700, 760 nm, respectively were turned on at 0s, 20s and 40s, respectively.

SPSD was evaluated using LEDs with different central wavelengths as the light source. The three LEDs, with central wavelengths at 630, 700, and 760 nm, respectively, were turned on in sequence. The time-dependent input optical power densities, as well as the induced photocurrents of SPSD were recorded. The results in Fig. S3 indicated that each TPCC layer could sense wavelengths better fitting its perovskite film's bandgap and corresponding to its center wavelength.

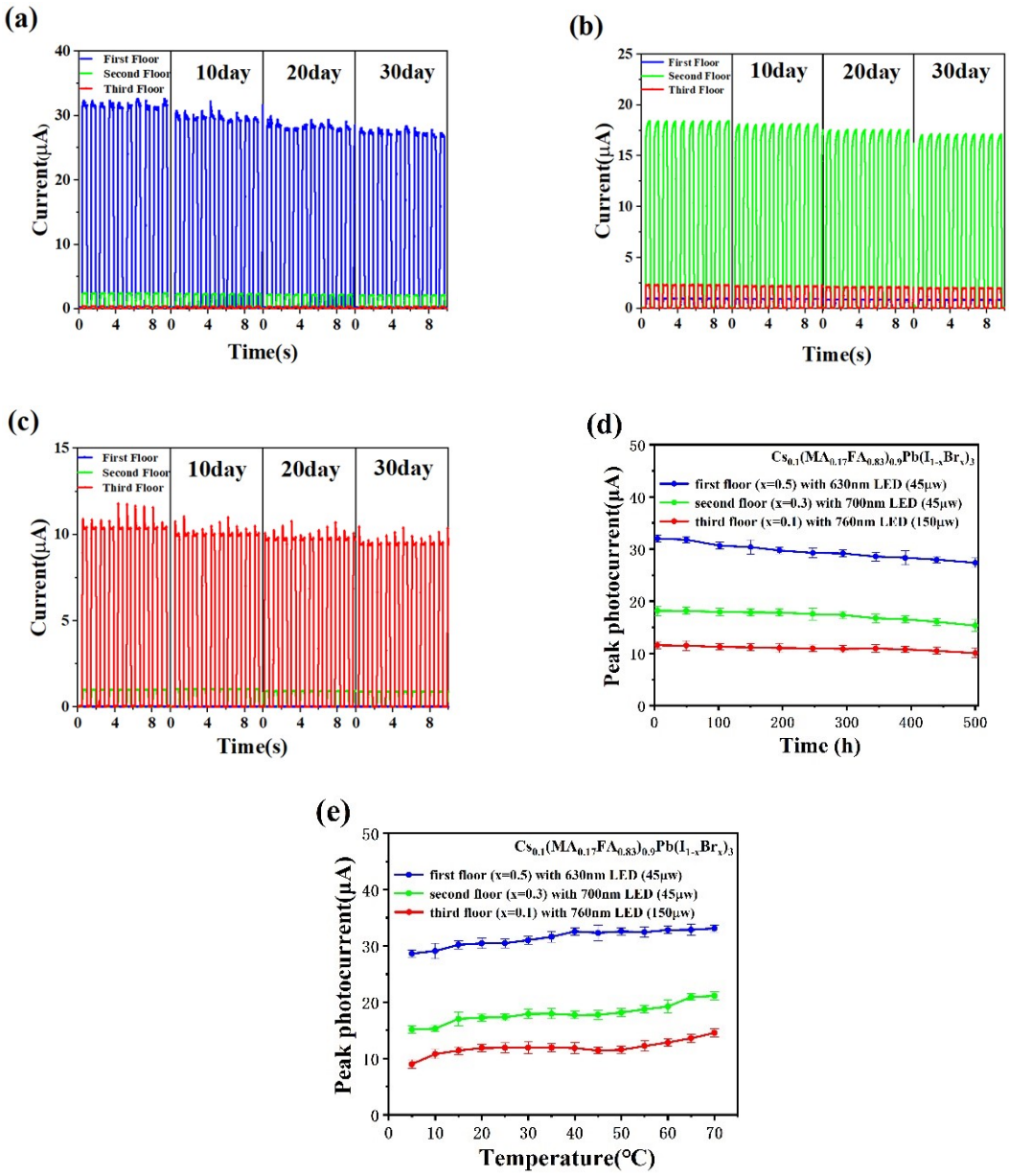

Fig. S4. The photocurrents of each TCPP layer in a SPSD device under the periodic light irradiation of (a) 630 nm (45 μw/cm^2), (b) 700 nm (45 μw/cm^2), and (c) 760 nm (150 μw/cm^2) after the device was stored in air for 10, 20 and 30 days at 25℃ and relative humidity 50%. (d) Dependence of the peak photocurrents of each TCPP in a SPSD device over time in ambient conditions at 50℃and relative humidity 50%. (e) The peak photocurrents of each TCPP in a SPSD device at temperature from 5-70℃ with a step of 5℃, and the relative humidity keeps 50%.

The as-fabricated SPSDs were stored at room temperature 25℃ and relative humidity 50% for 10, 20, and 30 days. Fig. S4(a)-(c) showed the photocurrents of each TCPP layer in a SPSD device

stored for 10, 20 and 30 days. The SPSD didn't show significant degradation even after 30 days' storage. It can be seen from Fig. S4(d) that SPSD has good stability at 50℃ and relative humidity of 50% for 500 hours. As shown in Fig. S4(e), the photocurrent of SPSD does not change abruptly with varied temperature.

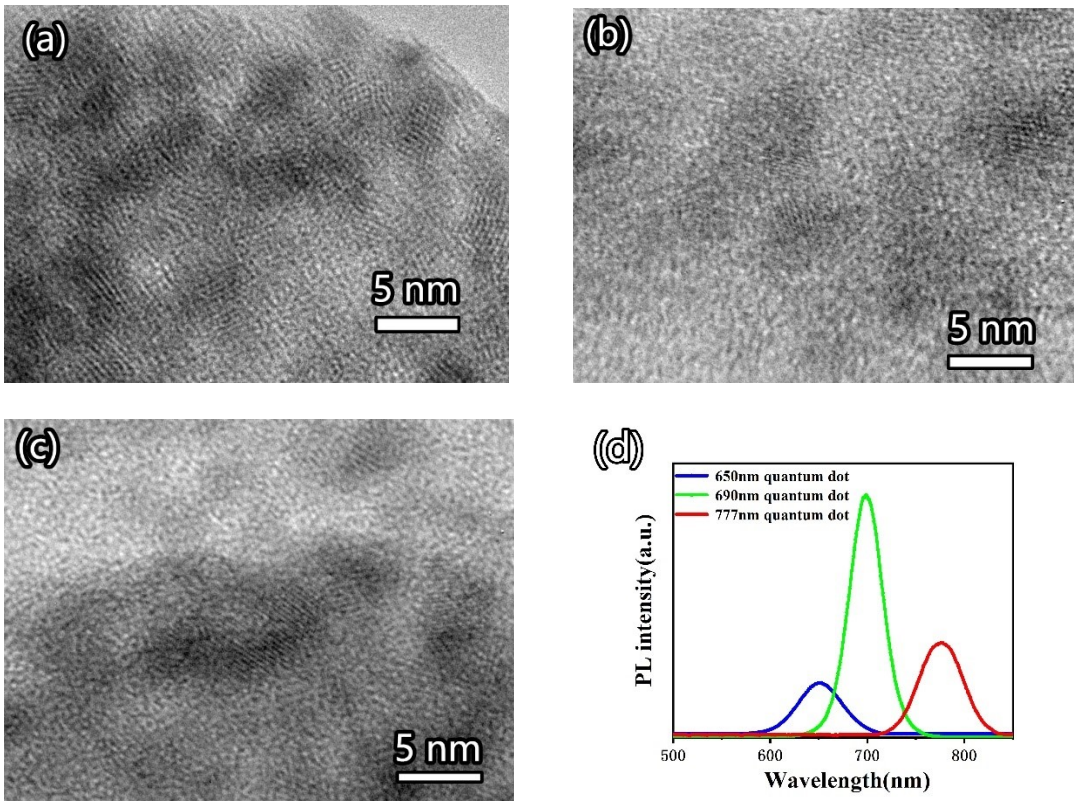

Fig. S5. TEM image of the CdTe quantum dots with different emission peak wavelength, (a) 650 nm, (b) 690 nm, (c) 777 nm. (d) The photoluminescence (PL) spectra of three kinds of QDs.

As shown in Fig. S5, the morphology and fluorescent features of the CdTe QDs (Xingzi, China) were measured by TEM, PL spectroscopy, respectively. It can be seen that the particle size distributed in the range of 3-8 nm and the three kinds of QDs shows three corresponding emission peaks at 650, 690, and 777 nm, respectively.